Available online at www.sciencedirect.com
SCIENCE DIRECT®
Journal of Nuclear Materials 329–333 (2004) 1515–1519
journal of nuclear materials
www.elsevier.com/locate/jnucmat

Surface roughening and grain orientation dependence of the erosion of polycrystalline stainless steel by hydrogen irradiation

M. Balden [a,*], A.F. Bardamid [b], A.I. Belyaeva [c], K.A. Slatin [c], J.W. Davis [d], A.A. Haasz [d], M. Poon [d], V.G. Konovalov [e], I.V. Ryzhkov [e], A.N. Shapoval [e], V.S. Voitsenya [e]

[a] *Max-Planck-Institut für Plasmaphysik, EURATOM Association, Boltzmannstr. 2, D-85748 Garching, Germany*
[b] *T. Shevchenko National University, 01033 Kiev, Ukraine*
[c] *National Technical University 'KhPI', 61108 Kharkov, Ukraine*
[d] *Fusion Research Group, University of Toronto Institute for Aerospace Studies, 4925 Dufferin St., Toronto, ON, Canada M3H 5T6*
[e] *NSC KIPT, 61108 Kharkov, Ukraine*

Abstract

Surface roughening of polycrystalline stainless steel mirrors due to hydrogen bombardment was studied as a function of ion fluence and energy ($1–4.3\times10^{24}$ H/m^2, 300–1500 eV/H). A strong micro-relief (100 nm scale) on single grains and a strong variation of the erosion depth between different grains were observed by scanning electron microscopy (SEM). A broad variation of the in-grain micro-relief was found to be independent of impact energy. The sputtering yield (Y) depends on the grain orientation, varying by a factor of about 2 for all impact energies. The correlation between surface morphology and orientation of the single grains was investigated using electron backscattering diffraction (EBSD). Grains with nearly (1 1 1) surface orientation do not show any significant in-grain micro-relief, although they have nearly the highest Y. For other orientations close to low indexed surfaces, e.g., (3 1 1), no correlation was found between Y and roughness.

1. Introduction

Plasma behaviour during fusion reactor operation requires a variety of diagnostics; for examples, see [1]. Among these are many optical methods which are successfully used in current fusion plasma experiments. In a fusion reactor environment all optical methods must be based on reflective – not refractive – optics, requiring the use of mirrors. The mirror surface has to withstand the sometimes harsh conditions, e.g., bombardment by charge exchange (CX) neutrals of a broad energy distribution, neutrons and high X-ray doses [2]. It is inevitable that the optical properties of the mirror will degrade under these conditions. A number of studies dealing with the topic of specifying these conditions and determining the degradations of the mirrors are available, e.g., [3].

In studies of the influence of the particle impact with various energies, rough surface morphologies were observed [4–8]. The surface roughness leads to changes in the optical properties of the mirror [7,8]. The objective of the present study is to investigate the correlation between grain orientation and erosion morphology. Should a particular grain orientation be more resistant to ion bombardment with respect to degradation of optical properties, single crystal mirrors with the desirable

* Corresponding author. Tel.: +49-89 3299 1688; fax: +49-89 3299 1212.
E-mail address: martin.balden@ipp.mpg.de (M. Balden).

0022-3115/$ - see front matter © 2004 Elsevier B.V. All rights reserved.
doi:10.1016/j.jnucmat.2004.04.240

surface orientation could be recommended for reactor use.

2. Experimental

2.1. Sample material, erosion treatment and optical characterisation

The specimen used in the study was cut from a sheet of polycrystalline austenitic stainless steel (4Cr16Ni11-Mo3Ti – similar to SS316) to a size of $22\times22\times3$ mm^3. It was then mechanically polished to a high optical quality.

The hydrogen ion irradiation of the specimen was performed at the University of Toronto, using a mass-separated H_3^+ ion beam. The ion accelerator system is similar to the one described in [9]. To restrict the spatial flux variation of the ion beam within a factor of 2, a mask with a 3-mm diameter aperture was mounted directly onto the specimen.

In order to investigate the dependence of the creation of surface morphology of the mirror on ion impact energy and fluence, nine different H_3^+ irradiations (with normal incidence) at room temperature were performed. The nine cases include the combination of three different ion energies (300, 650 and 1500 eV/H) and three different ion fluences (1.1, 2.2–2.9, and 4.3×10^{24} H/m^2); see Table 1.

The characterisation of the optical properties in the sputtering spots was performed by ellipsometry and reflectance measurements, which were reported in [7] and compared to non-exposed surface parts of the specimen. (More optical characterisation was performed on similarly prepared specimens [8].)

2.2. Surface morphology and crystal orientation studies by EBSD

The irradiated specimen studied here was previously analyzed for surface features and spectral reflectance using scanning electron microscopy (SEM) and ellipsometry, respectively [7]. In the present study, higher magnifications were performed with SEM (Philips XL30 ESEM) to focus on some of the details of the surface morphology. Furthermore, the grain, i.e., crystallite, orientation was studied by electron back scattering diffraction (EBSD; HKL Technology) using the electron beam in the SEM apparatus.

A brief description of the EBSD technique with its limitation is given here. More detailed information can be found elsewhere, e.g., [11,12].

The diffuse back-scattered electrons are partly diffracted on the crystal lattice. Therefore, a very small modulation of the spatial distribution of the back-scattered electrons occurs. This spatial distribution is produced by an electron beam with a large incident angle to the surface normal (60–80°) and is made visible on a fluorescent screen which is recorded by a CCD camera. With image processing (e.g., background subtraction), the diffraction 'line' pattern (Kikuchi pattern [11]) is extracted and compared with calculated ones. The lattice parameters of the investigated crystal phases are necessary for the calculation (here: fcc lattice with 0.365 nm lattice constant) and the geometrical set-up has to be calibrated on a crystal with known orientation, e.g., using the cleaved edge of Si(1 0 0) wafer. The diffraction pattern is fixed with the lattice. An orientation change, i.e., rotation of the crystallite, causes a defined change in the pattern. In the analysis, the lattice for the calculated pattern is rotated until the best fit with the observed pattern is reached. (If the fit is bad, the data point is specially marked.) So, the full orientation matrix is known, and could be expressed, for example, in Euler angles with respect to the calibrated specimen co-ordinate system.

For orientation microscopy the electron beam is scanned – as is done for SEM images. The EBSD pattern are obtained at each scan position and an analysis, as described above, is performed. Therefore, an orien-

Table 1
Erosion conditions and properties of the erosion spots

Spot no.	Energy (eV)	Sputtering yield [10]	Fluence (10^{24} H/m^2)	Calculated average erosion depth (μm)	Maximum observed step height (μm)	Visibility of erosion morphology
#3	300	0.007	1.1	0.10	–	Very weak
#2			2.2	0.19	–	Weak
#1			4.3	0.38	0.25	Good
#6	650	0.013	1.1	0.18	–	Very weak
#5			2.2	0.36	–	Good
#4			4.3	0.71	0.2	Good
#9	1500	0.015	1.1	0.21	–	Good
#8			2.9	0.55	–	Good
#7			4.3	0.82	0.5	Good

tation mapping with good signal to noise ratio for each pattern requires measurements over several hours. The relative error of the orientation in a mapping is usually about 1°. Due to the uncertainty introduced by the calibration of the geometry, the total error of the orientation is about 2° [11,12].

The lateral resolution of EBSD orientation mapping depends on the size of the interaction volume of the primary electron beam with the specimen. This volume is mainly defined by the primary electron energy, impact angle (specimen tilting), and specimen material. (Tilting of 75° and an electron energy of 20 keV were used in this study.) Due to the strong tilting (~60–80° from the surface normal) the lateral resolution perpendicular to the tilt axis is about 3 times worse than it is for the parallel direction, but it is still smaller than 1 μm, see in [11,12]. The effective resolution in the images is even better [11,12]. The small modulation of the spatial distribution of the back-scattered electrons is produced only in the last nanometers near the surface of the crystal, because the diffracted electrons can only survive a few nm before they lose their direction due to other scatter events. Therefore, a distorted surface, e.g., by polishing, destroys the pattern. The strong tilting is mainly necessary to increase the modulation above the detection limit [11].

3. Results

Figs. 1 and 2 show typical erosion morphologies for H_3^+ irradiation at 300 and 1500 eV/H after an ion fluence of 4.3×10^{24} H/m^2 (#1, #7). In both images of Fig. 1 only a few grains are visible. The individual grains are nearly always separated by steps. These stepped relief features result from the different erosion rates of the differently orientated grains [4,5,13]. Some grains still have smooth surfaces, while other surfaces are strongly roughened (in-grain micro-relief). Such roughening has been already previously reported [4–8]. (Furthermore, ion etching, i.e., ion impact, is a standard preparation technique in metallography to visualise the grain structure of polycrystalline materials, see e.g., [14].) Even from the small number of grains observed in Fig. 1, but also from the images of Figs. 2 and 3(a) with lower magnification, it can be concluded that the formation of a smooth or rough surface is not correlated with a low or high sputtering yield of an individual grain.

By analysing large numbers of grains in tilted and untilted SEM geometry, the maximum observed step height is determined for three erosion spots, see Table 1. The calculated average erosion depth, based on irradiation fluence and sputtering yield [10], is also given in Table 1. By studying the image of scratches in tilted and untilted geometry, the erosion depth close to the spot boundary of spot #7 could be determined to be

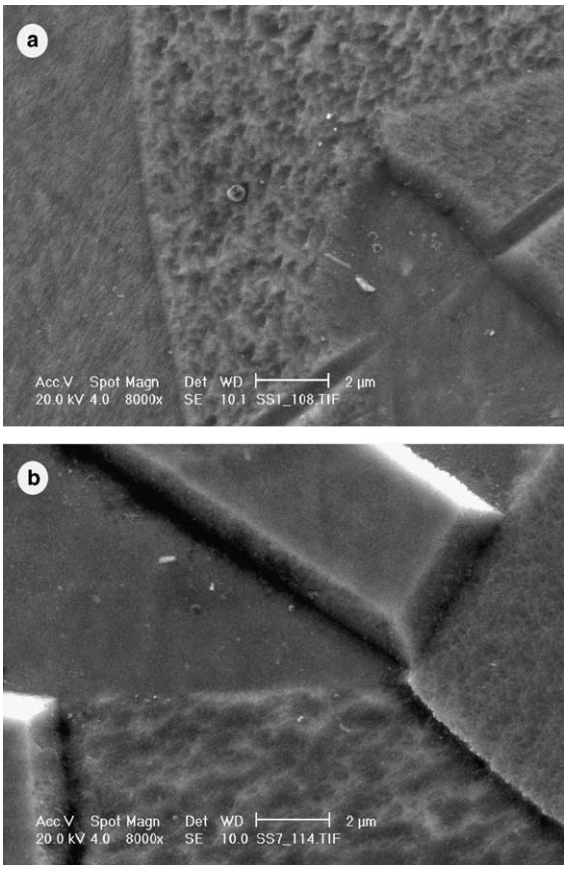

Fig. 1. Typical erosion morphology in high magnification SEM of a specimen irradiated with a fluence of 4.3×10^{24} H/m^2 with ion impact energies of: (a) 300 eV/H (#1) and (b) 1500 eV/H (#7).

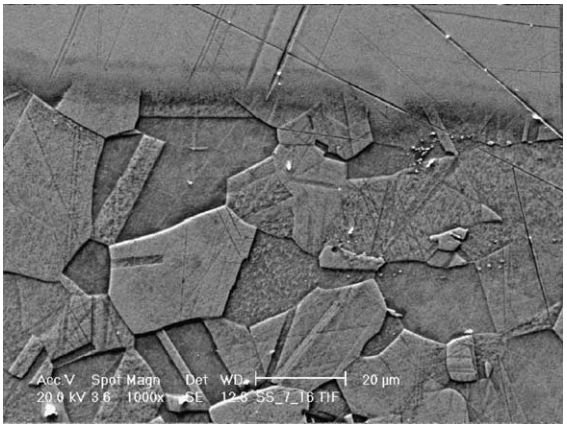

Fig. 2. SEM image of spot #7 after irradiation by 1500 eV/H to a fluence of 4.3×10^{24} H/m^2. The spot boundary is visible in the top of the image.

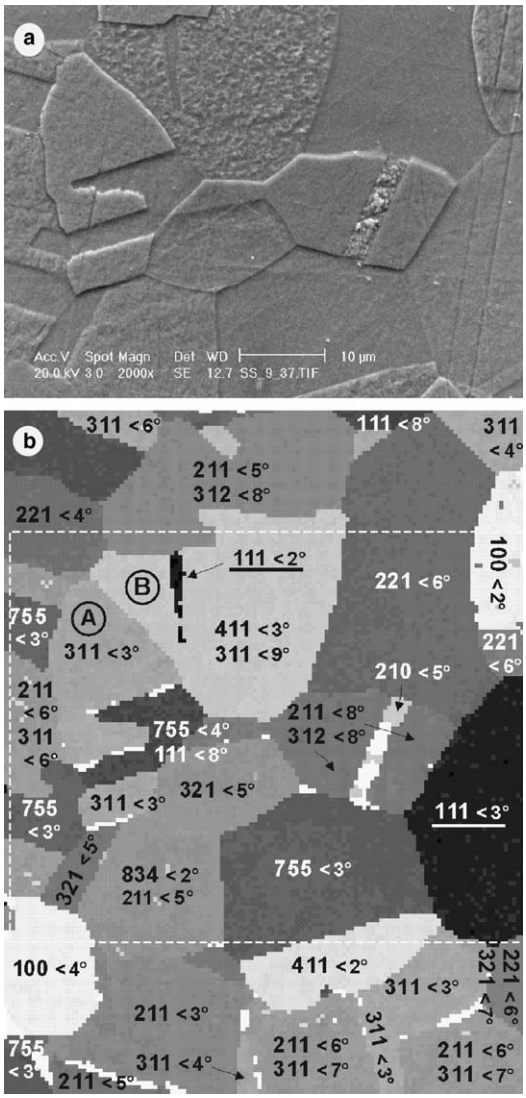

Fig. 3. (a) SEM image and (b) grain orientation mapping determined from EBSD for 1500 eV/H irradiation to a fluence of 1.1×10^{24} H/m^2 (#9). The image area of (a) is included in the middle of (b); dotted rectangle. The grey scale of (b) is defined as the angle between surface normal and the ⟨111⟩ direction. Black represents the angle 0°, i.e., grains in black have the (1 1 1) orientation (white: unsolved EBSD pattern). Other low index surfaces are also labelled. The angles after the orientation numbers represent the average derivation from a particular surface. For the orientation mapping a lateral step width of 0.5 μm was used.

~0.7 μm. This value is in reasonable agreement with the calculated averaged erosion depth.

By investigating the spot boundaries (e.g., Fig. 2) it is also possible to estimate the thickness of the distorted surface layer which was created during the sample polishing procedure. This layer appears as a misty region along the spot boundary, where the grain boundaries vanish (Fig. 2, upper part). The quality of the EBSD 'line' pattern is used as the criterion, where still the distorted layer is present and where not. From the lateral position of suitable EBSD pattern and by studying scratches across the spot boundary in tiled and untilted geometry, the thickness of the distorted layer is estimated to be 0.1–0.2 μm. This thickness is consistent with the calculated average erosion depth corresponding to the appearance of visible erosion morphology (Table 1). Keeping the distorted layer in mind and comparing the average erosion depth with the maximum observed step height, it could be concluded that sputtering yields for different individual grains change by a factor of about 2 for all energies. Such a spread in the sputtering yield is well known for several fcc metals, like Cu, Ag, and Ni [13,15]. Usually the spread varies with impact energy. For example, the ratio of the sputtering yield of Cu(1 1 1) to Cu(1 1 0) bombarded with Ar ions reaches a maximum at about 5 keV ($Y_{111}\approx3\times Y_{110}$) [13].

In examining the in-grain micro-relief – ranging from 'crater-like depressions' to 'packed fine fibre-like' features – no correlation is evident with the impacting H ion energy. The creation of such mirco-relief is investigated for decades (e.g., [4–6]) and in recent studies nanostructuring was emphasised (e.g., [16]). Also several theoretical approaches describe this micro-roughening [17,18]. Nevertheless, more than half of all observed grains have 'smooth' surfaces, i.e., no structure with size above 50 nm (see Fig. 1).

Fig. 3(b) shows an EBSD orientation mapping. The grey scale is defined as the angle between the surface normal and the ⟨1 1 1⟩ direction of the crystal lattice. Grains with a (1 1 1) surface appear black. Other low index surfaces are also labelled. The angles after the orientation numbers represent the average derivation from this particular surface. By comparing the erosion morphology with the grain orientation (Fig. 3(a) and (b)), it is evident that the (1 1 1) surface stays smooth during the erosion. On the other hand, the (1 1 1) orientated grains do not have the lowest sputtering yield; in fact they appear to have the highest one [13] (see the edges of the (1 1 1) grain at the right border of Fig. 3). Similar observations are noted for all surface areas analyzed. Studies with Mo mirrors, exposed to a deuterium plasma, also show that the densest face – the (1 1 0) orientation for bcc lattice structure – have the highest smoothness [19], and the highest sputtering yield [13].

For other orientations close to low indexed surfaces no relation to the in-grain mirco relief and to the sputtering yield is found. As an example the (3 1 1) grain marked with A in Fig. 3(b) is smooth, while another (3 1 1) grain (not in the area of Fig. 3) has an in-grain mirco relief comparable to that of grain B.

4. Conclusion

Surface analysis of stainless steel subsequent to H_3^+ irradiation shows that the erosion yield of individual grains (with different orientation) varies by a factor of about 2 for all energies. This produces large erosion depth variations and the typical stepped micro-relief structure. While more than half of the grains have smooth surfaces, the others contain a broad variety of in-grain micro-relief ranging from 'crater-like depressions' to 'packed fine fibre-like' features.

Grains with (1 1 1) surface orientation do not show significant in-grain micro-relief, although they do not have the lowest sputtering erosion yield. Small variations of the angle (several degrees) between the ion impact direction and low indexed planes, e.g., (3 1 1), lead to strong changes in the erosion yield and to the creation of different in-grain micro-relief features.

References

[1] P.E. Stott, G. Gorini, E. Sindoni (Eds.), Diagnostics for Experimental Fusion Reactor, Plenum, New York, 1996.
[2] D.V. Orlinski, Radiation hardening of diagnostic components, Ref. [1], p. 51.
[3] V. Voitsenya, A.E. Costley, V. Bandourko, et al., Rev. Sci. Instrum. 72 (2001) 475.
[4] R. Behrisch (Ed.), Sputtering by Particle Bombardment II, Topics in Applied Physics, vol. 54, Springer, Berlin, 1983.
[5] R. Behrisch, K. Wittmark (Eds.), Sputtering by Particle Bombardment III, Topics in Applied Physics, vol. 64, Springer, Berlin, 1991.
[6] G.H. Wehner, J. Vac. Sci. Technol. A 3 (1985) 1821.
[7] A.F. Bardamid, A.I. Belyaeva, V.N. Bondarenko, J.W. Davis, A.A. Galuza, I.E. Garkusha, A.A. Haasz, V.G. Konovalov, A.D. Kudlenko, M. Poon, I.V. Ryzhkov, S.I. Solodovchenko, A.F. Shtan, V.S. Voitsenya, K.I. Yakimov, Phys. Scr. T 103 (2003) 109.
[8] A.I. Belyaeva, A.F. Bardamid, J.W. Davis, A.A. Haasz, S.N. Kolomiets, V.G. Konovalov, A.D. Kudlenko, M. Poon, V.S. Voitsenya, J. Nucl. Mater., submitted for publication.
[9] A.A. Haasz, J.W. Davis, Nucl. Instrum. and Meth. B 83 (1993) 117.
[10] Y. Yamamuram, H. Tawara, ADNDT 62 (1996) 149.
[11] V. Randle, O. Engler, Introduction to Texture Analysis: Macrotexture, Microtexturwe and Orientation Mapping, Taylor & Francis, London, 2002.
[12] F.J. Humphreys, J. Mater. Sci. 36 (2001) 3833.
[13] H.E. Rosendaal, in: R. Behrisch (Ed.), Sputtering by Particle Bombardment I, Topics in Applied Physics, vol. 47, Springer, Berlin, 1981.
[14] I. Gräf, Practical Metallogr. 35 (1998) 235, 316, 359 and 38 (2001) 287, 617, 699.
[15] I.N. Evdokimov, V.E. Yurasova, Poverkhnost 9 (1988) 5 (in Russian).
[16] J.F. Whitacre, Z.U. Rek, J.C. Bilello, S.M. Yalisove, J. Appl. Phys. 84 (1998) 1346.
[17] M. Küstner, W. Eckstein, V. Dose, J. Roth, Nucl. Instrum. and Meth. B 145 (1998) 320.
[18] M. Stepanova, S.K. Dew, I.P. Soshnikov, Phys. Rev. B 66 (2002) 125407.
[19] A.F. Bardamid, V.G. Konovalov, I. Orlovsky, I.V. Ryzhkov, A.N. Shapoval, A.F. Shtan, S.I. Solodovchenko, V.S. Voitsenya, K. Yu. Vukolov, K.I. Yakimov, Paper 2–10 at the International Conference and School on Plasma Physics and Controlled Fusion (Alushta, Crimea, Ukraine, September 2002), Plasma Dev. Oper., submitted for publication.